analytical chemistry

pubs.acs.org/ac Article

Multiplexable and Biocomputational Virus Detection by CRISPR-Cas9-Mediated Strand Displacement

Rosa Márquez-Costa,[#] Roser Montagud-Martínez,[#] María-Carmen Marqués, Eliseo Albert, David Navarro, José-Antonio Daròs, Raúl Ruiz, and Guillermo Rodrigo*

Cite This: https://doi.org/10.1021/acs.analchem.3c01041 Read Online

ACCESS | Metrics & More | Article Recommendations | Supporting Information

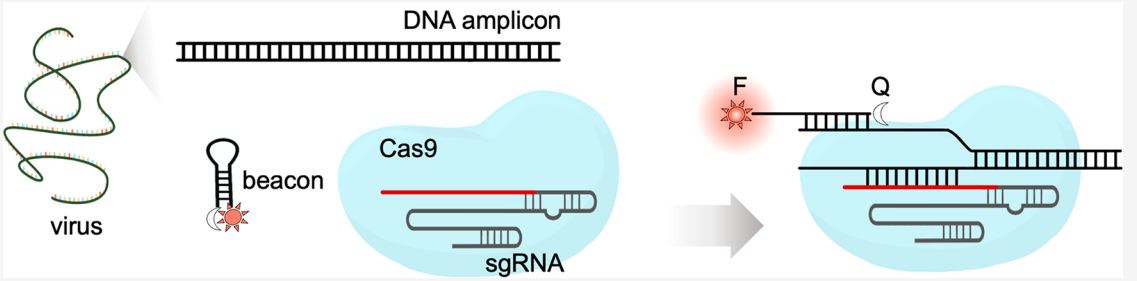

ABSTRACT: Recurrent disease outbreaks caused by different viruses, including the novel respiratory virus SARS-CoV-2, are challenging our society at a global scale; so versatile virus detection methods would enable a calculated and faster response. Here, we present a novel nucleic acid detection strategy based on CRISPR-Cas9, whose mode of action relies on strand displacement rather than on collateral catalysis, using the *Streptococcus pyogenes* Cas9 nuclease. Given a preamplification process, a suitable molecular beacon interacts with the ternary CRISPR complex upon targeting to produce a fluorescent signal. We show that SARS-CoV-2 DNA amplicons generated from patient samples can be detected with CRISPR-Cas9. We also show that CRISPR-Cas9 allows the simultaneous detection of different DNA amplicons with the same nuclease, either to detect different SARS-CoV-2 regions or different respiratory viruses. Furthermore, we demonstrate that engineered DNA logic circuits can process different SARS-CoV-2 signals detected by the CRISPR complexes. Collectively, this CRISPR-Cas9 R-loop usage for the molecular beacon opening (COLUMBO) platform allows a multiplexed detection in a single tube, complements the existing CRISPR-based methods, and displays diagnostic and biocomputing potential.

INTRODUCTION

Infectious diseases defy the modern lifestyle of our societies, and it is increasingly evident that better and handier detection methods of viruses and bacteria would facilitate their control. Of note, the coronavirus disease 2019 (COVID-19) pandemic caused by severe acute respiratory syndrome coronavirus 2 (SARS-CoV-2)[1] has highlighted the challenges in diagnostics of viral infections. A fast and confident diagnostic tool contributes to significantly reducing the transmission of the virus in the community and allows early therapeutic actions that can mitigate acute outcomes of infection. Currently, a reverse transcription quantitative polymerase chain reaction (RT-qPCR) is the gold-standard diagnostic technique of infectious diseases in the clinic due to its high sensitivity and specificity.[2] However, when a rapid and massive intervention is required, such as in a pandemic context, alternative techniques that can bypass, at least in part, the need for expensive equipment and well-trained personnel are highly required.[3]

Clustered regularly interspaced short palindromic repeat (CRISPR) systems are being repurposed in recent years for diagnostic applications.[4,5] Owing to the ability of some CRISPR-associated (Cas) proteins to display a collateral catalytic activity upon target recognition, a sensitive and specific nucleic acid detection is possible. In combination with isothermal amplification techniques,[6] sensitivities at the attomolar scale (i.e., about one copy per microliter) and specificities at one nucleotide resolution have been achieved, atop of bypassing the dependence on qPCR equipment. In this regard, the use of CRISPR systems may represent a suitable alternative for the diagnostics of infectious diseases in the clinic and also in the field. Notably, these systems have been already applied to detect SARS-CoV-2 in clinical samples.[7] Indeed, different assays based on CRISPR-Cas12[7−9] or CRISPR-Cas13[10−12] have been implemented for the detection of SARS-CoV-2 (even the direct detection of the virus without

Received: March 8, 2023
Accepted: May 5, 2023

https://doi.org/10.1021/acs.analchem.3c01041
Anal. Chem. XXXX, XXX, XXX−XXX

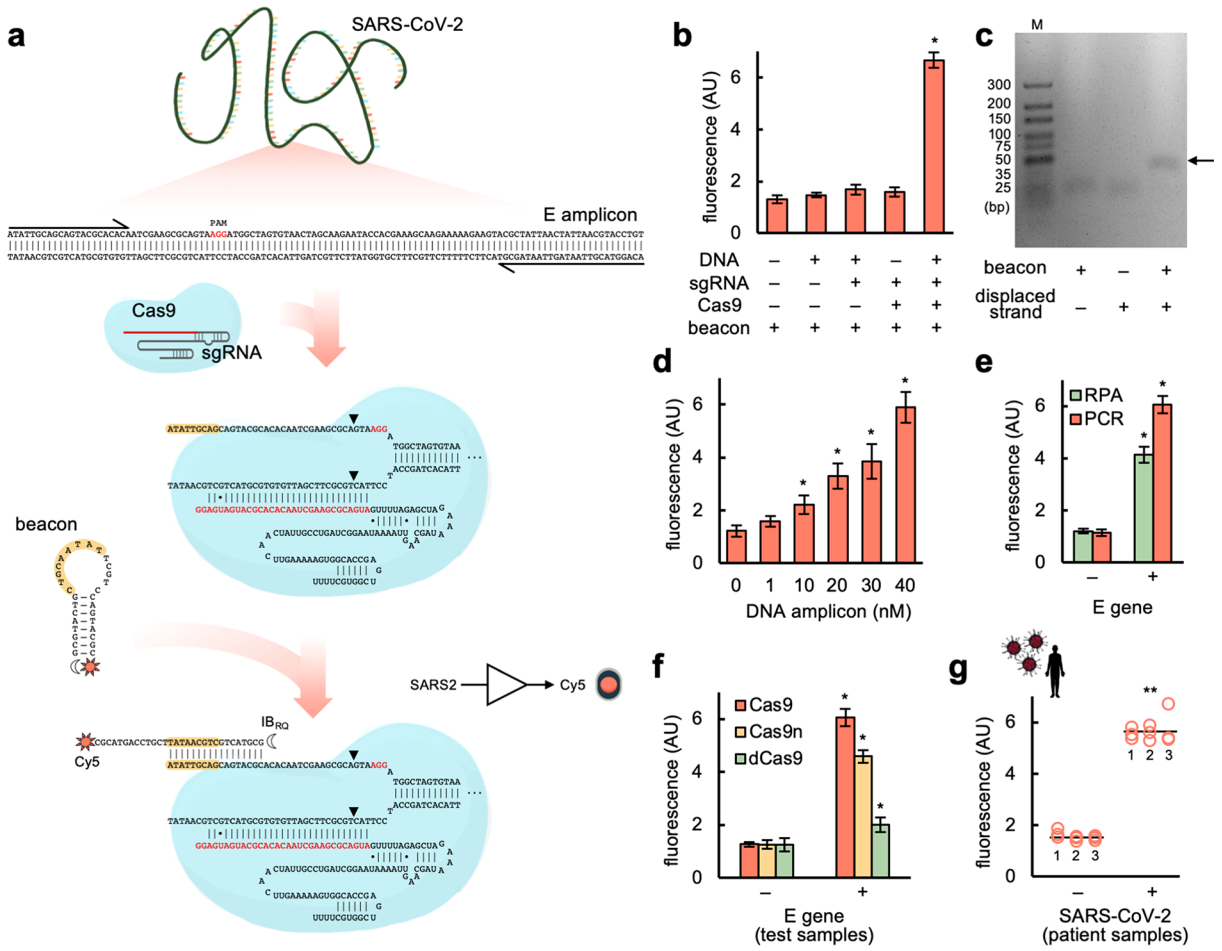

Figure 1. SARS-CoV-2 detection through a CRISPR-Cas9-based strand displacement reaction. (a) Schematics of the global reaction of amplification and detection of a DNA product from SARS-CoV-2 E gene (PCR primers drawn at the ends), containing a PAM (shown in red) for Cas9 recognition. A preassembled CRISPR-Cas9 ribonucleoprotein targeting the amplicon (sgRNA spacer marked in red) was then able to displace a strand so that the molecular beacon could interact with and change its conformation (seed region for this interaction marked in yellow). The molecular beacon was labeled with the fluorophore Cy5 (sun icon) in the 3′ end and the dark quencher IB_{RQ} (moon icon) in the 5′ end. Wobble base pairs denoted by dots. (b) Fluorescence-based characterization of the detection; amplifications performed by PCR. (c) Gel electrophoretic assay to reveal the interaction between the molecular beacon and the displaced strand from the DNA amplicon (the arrow marks the intermolecular complex). M, molecular marker. (d) Effect of the DNA amplicon concentration on the output fluorescence signal. (e) Detection of the DNA amplicon generated by PCR or RPA (isothermal method). (f) Effect of different versions of Cas9 (Cas9, Cas9n, or dCas9) on the output signal. (g) Detection of SARS-CoV-2 in patient samples (6 patients, 3 reactions per patient); amplifications performed by RT-PCR. Error bars correspond to standard deviations (n = 3). *Statistical significance with test samples (Welch's t-test, two-tailed $P < 0.05$). **Statistical significance with patient samples (Welch's t-test, two-tailed $P < 0.001$).

preamplification has been possible with the *Leptotrichia buccalis* Cas13a nuclease).[12] However, the multiplexed detection remains challenging due to the nonspecificity of that collateral catalytic activity. Certainly, sensing different elements at a time can be of utility for determining the presence of coinfecting pathogens or even for genotyping and identifying diverse mutations.

To overcome this limitation, orthogonal Cas proteins can be employed to achieve multiplexed nucleic acid detection in a single reaction (e.g., by using a Cas12 to target DNA and a Cas13 to target RNA).[13] Nevertheless, the number of nucleic acids that can be detected simultaneously is limited by the number of different Cas proteins involved in the assay. The use of droplets constitutes an alternative to distribute the detection by performing specific reactions in different compartments, thereby allowing a multiplexed detection with just one CRISPR system,[14] in addition to descending the limit of detection.[15] Moreover, a recent development exploited the formation of noncanonical CRISPR RNAs for multiplexed RNA detection with Cas9 revealed by gel electrophoresis.[16] In any case, we still need to develop further methods that are easy to implement for multiplexed nucleic acid detection, especially to achieve point-of-care applications in emergency scenarios.

In this work, we present a novel nucleic acid detection approach based on CRISPR-Cas9 aimed at fulfilling the aforementioned gap. We exploited the absence of the collateral catalytic activity of *Streptococcus pyogenes* Cas9 to develop a simple procedure based on CRISPR-mediated strand displacement[17] and fluorogenic molecular beacons[18] that allows a direct multiplexed detection of nucleic acids in a single tube. We called this platform COLUMBO (CRISPR-Cas9 R-loop usage for molecular beacon opening). First, we demonstrate that this can be applied to detect SARS-CoV-2. Second, we demonstrate a simultaneous detection of three different genomic regions of this coronavirus, as well as the potential application of detecting three different viruses in the sample or

https://doi.org/10.1021/acs.analchem.3c01041
Anal. Chem. XXXX, XXX, XXX−XXX

even discriminating SARS-CoV-2 variants without the need for sequencing. Third, we couple the detection of SARS-CoV-2 to DNA-based computation.

RESULTS

Rational Design of COLUMBO. COLUMBO requires a preamplification step to generate a suitable double-stranded DNA fragment from the nucleic acid of interest (DNA or RNA). This can be done by PCR or by an alternative method running isothermally, such as recombinase polymerase amplification (RPA).[19] Importantly, the amplified DNA molecule needs to harbor a protospacer adjacent motif (PAM) for Cas9 binding (NGG). Then, the sequence-specific detection is accomplished thanks to interfacing a CRISPR-Cas9 reaction with an appropriately designed molecular beacon (single-stranded DNA, ssDNA) folding into a stem-loop structure. Once the R-loop is formed, the nontargeted DNA strand that has been displaced can interact with other nucleic acids supplied in *trans*.[20] Previously, we showed that this mechanism is instrumental to engineer toehold-free DNA circuits for logic computation.[17] Here, the interaction of the beacon with the displaced strand causes the reconfiguration of the former separating the fluorophore from the quencher, thereby producing a fluorescent signal (Figure 1a).

We envisioned a system in which the PAM-distal region of the displaced strand is responsible for the interaction with the beacon. This interaction is seeded by the pairing of some nucleotides located in the loop of the beacon with the complementary nucleotides located in the 5′ end of the displaced strand, ensuring a low activation energy barrier.[21] The beacon is not fully complementary to the displaced strand (only one-half binds to it). Moreover, to limit the potential interaction of the beacon with the single guide RNA (sgRNA), the spacer of the sgRNA excludes the seed region of the displaced strand. The spacer also harbors a mutation in the 5′ end region to form a wobble base pair with the targeted DNA strand.[22] The R-loop opens spontaneously at the PAM-distal region as a result of a low melting temperature, thereby exposing the 5′ end of the displaced strand to the solvent. Consequently, the beacon only opens when the ternary CRISPR complex (DNA-sgRNA-Cas9) is formed (Figure S1).

SARS-CoV-2 Detection with COLUMBO. Using the Charité (Berlin) E-Sarbeco primers,[23] we generated a suitable DNA amplicon for COLUMBO by PCR from a test sample based on the SARS-CoV-2 E gene. The amplified material was purified to remove elements potentially interfering with the molecular beacon. An sgRNA was designed to exploit a PAM located at an appropriate position (Figure 1a), in vitro transcribed from a DNA template, and assembled with a Cas9 given from a commercial preparation. In turn, a molecular beacon appropriately designed was chemically synthesized, labeling its 3′ end with the fluorophore cyanine 5 (Cy5) and its 5′ end with the dark quencher Iowa Black RQ (IB_{RQ}). Then, we added the sgRNA-Cas9 ribonucleoprotein to the reaction to target the amplified DNA (detection of the nucleic acid of interest) and the beacon to produce a red fluorescent signal upon interaction with the displaced strand in the PAM-distal region. Remarkably, COLUMBO displayed good performance, with a dynamic range of more than 3-fold change in red fluorescence and no apparent opening of the beacon in response to the DNA amplicon or the sgRNA alone (Figure 1b). The ability of the beacon to interact with the displaced strand was also assessed by agarose gel electrophoresis (Figure 1c). Furthermore, we performed a set of reactions with increasing concentrations of the DNA amplicon, observing proportionality between the input and output signals (Figure 1d). Thus, COLUMBO might be used to quantify a given DNA in the sample ranging from the nanomolar scale.

Next, we tested the ability of using RPA instead of PCR to generate the DNA amplicon in combination with COLUMBO, as this is important to achieve point-of-care applications. Our results indicate that both methods are suitable, having used the very same primers (Figure 1e). A slightly higher fluorescent signal in the presence of the target DNA was produced after PCR, while the preamplification process was faster with RPA. In terms of sensitivity, 1 copy/μL in the sample was detected irrespective of the amplification method (Figure S2). In addition, we inspected the impact of the catalytic activity of Cas9 on the performance of COLUMBO. To this end, we used three different versions of Cas9: the wild-type nuclease, the Cas9 H840A nickase (Cas9n), which only cleaves the nontargeted strand, and the catalytically dead Cas9 protein (dCas9), which does not produce any cleavage.[24] Both Cas9 and Cas9n produced a substantial fold change in fluorescence upon detection, although higher in the case of Cas9 (Figure 1f). However, dCas9 failed in reaching such a performance, despite a significant differential readout was still possible. Arguably, the cleavage of the nontargeted strand confers more translational and rotational freedom to facilitate the interaction with the beacon.[25] We also found Cas9 and Cas9n to have equal activity on displacing that strand, but lower in the case of dCas9 (Figure S3). Motivated by these results, we decided to apply COLUMBO to detect SARS-CoV-2 in patient samples. Nasopharyngeal swabs from people diagnosed as positive or negative in viral infection by RT-qPCR in the hospital were collected.[26] We reconfirmed the infections by RT-qPCR in our lab (Figure S4). After RT-PCR amplification with the Charité E-Sarbeco primers (without RNA extraction), COLUMBO displayed marked differential readouts that were useful to discriminate the presence of the virus (Figure 1g). These results demonstrate the potential suitability of COLUMBO to perform clinical diagnostics in a simple and effective way.

Evaluation of Modifications of COLUMBO. To avoid the purification step after the preamplification reaction, the region targeted by the molecular beacon should distinguish from those targeted by the primers and the sgRNA. In this regard, a strategy based on cleaving the resulting DNA amplicon in the PAM-distal region with a restriction enzyme was devised (Figure S5). We achieved a successful detection with no apparent leakage following this approach (dynamic range of more than 2.5-fold in red fluorescence). In addition, we investigated the use of the PAM-proximal region of the displaced strand to interact with the molecular beacon. A new beacon targeting the N1 amplicon was designed. We found a significant opening of the beacon as a result of the interaction, but we also noticed an unwanted interaction with the sgRNA, which reduced the net dynamic range of the system (Figure S6).

Multiplexed SARS-CoV-2 Detection with COLUMBO. We then moved forward to perform the simultaneous detection of different genomic regions of SARS-CoV-2. This is important to minimize the rate of false positives. The Centers for Disease Control and Prevention (CDC) N1 and N2 primers[23] were used together with the Charité E-Sarbeco primers to generate three different DNA amplicons by PCR from a test sample based on the SARS-CoV-2 N and E genes.

https://doi.org/10.1021/acs.analchem.3c01041
Anal. Chem. XXXX, XXX, XXX−XXX

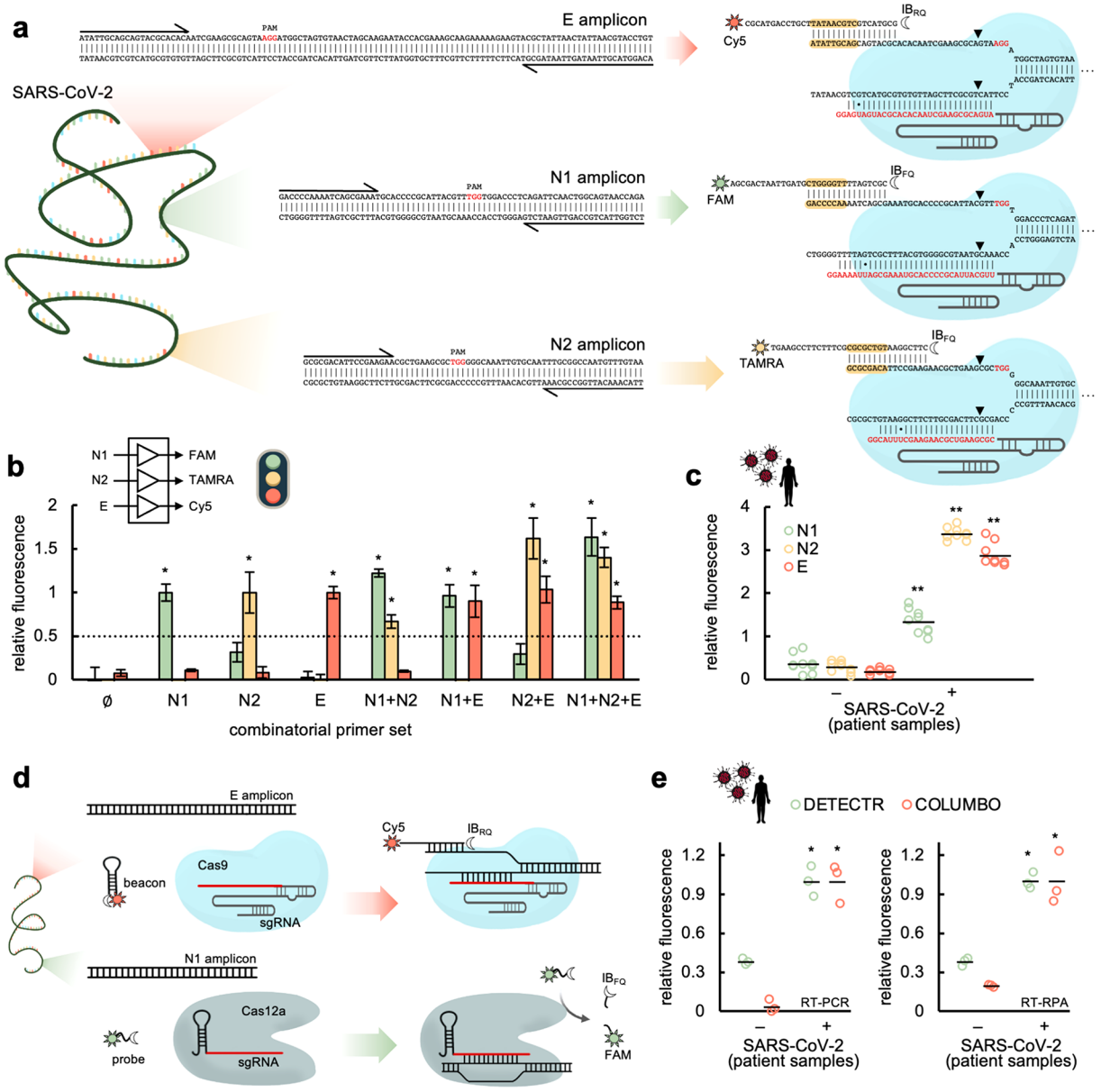

Figure 2. Multiplexed SARS-CoV-2 detection through CRISPR-Cas9-based strand displacement reactions. (a) Schematics of the global reactions of amplification and detection of three different DNA products from SARS-CoV-2 (from E and N genes, PCR primers drawn at the ends), containing each a PAM (shown in red) for Cas9 recognition. Preassembled CRISPR-Cas9 ribonucleoproteins targeting the amplicons (sgRNA spacers marked in red) and appropriate molecular beacons were used for the detection (seed regions for the beacon-displaced strand interaction marked in yellow). The molecular beacons were labeled with Cy5 and IB_{RQ} (for E detection), FAM and IB_{FQ} (for N1 detection), and TAMRA and IB_{FQ} (for N2 detection). Wobble base pairs denoted by dots. (b) Fluorescence-based characterization of the detection by performing amplifications with combinatorial sets of primers by PCR. The detection threshold (given by the dotted line) was set to 0.5, indicating that the difference in relative fluorescence was more than 2-fold. (c) Multiplexed detection of SARS-CoV-2 in patient samples (6 patients, 3 reactions per patient); amplifications performed by RT-PCR. (d) Schematics of the reaction of detection with COLUMBO and DETECTR of two different DNA products from SARS-CoV-2 (from E and N genes). A ssDNA probe labeled with FAM and IB_{FQ} was used for DETECTR (for N1 detection). (e) Fluorescence-based characterization of the detection by performing multiplexed amplifications by RT-PCR or RT-RPA (2 patients, 3 reactions per patient). Error bars correspond to standard deviations ($n = 3$). *Statistical significance with test samples (Welch's t-test, two-tailed $P < 0.05$, and relative fluorescence > 0.5). **/*Statistical significance with patient samples (Welch's t-test, two-tailed $P < 0.001/0.05$).

Suitable PAMs were found in these amplicons (Figure 2a). We designed the corresponding sgRNAs and molecular beacons according to the aforementioned specifications. The new beacons to detect the N1 and N2 amplicons were labeled with the fluorophores carboxyfluorescein (FAM) and carboxytetramethylrhodamine (TAMRA), respectively, in their 3′ end and with the dark quencher Iowa Black FQ (IB_{FQ}) in their 5′ end. No significant interferences were observed when using simultaneously these three fluorophores (Figure S7). Notably, COLUMBO allowed the precise detection of the different genomic regions having performed a series of combinatorial amplifications, with a minimal 3-fold change in relative fluorescence (Figure 2b). In addition, we performed a multiplexed RT-PCR amplification over patient samples with all primers. COLUMBO gave a positive signal in the three

https://doi.org/10.1021/acs.analchem.3c01041
Anal. Chem. XXXX, XXX, XXX−XXX

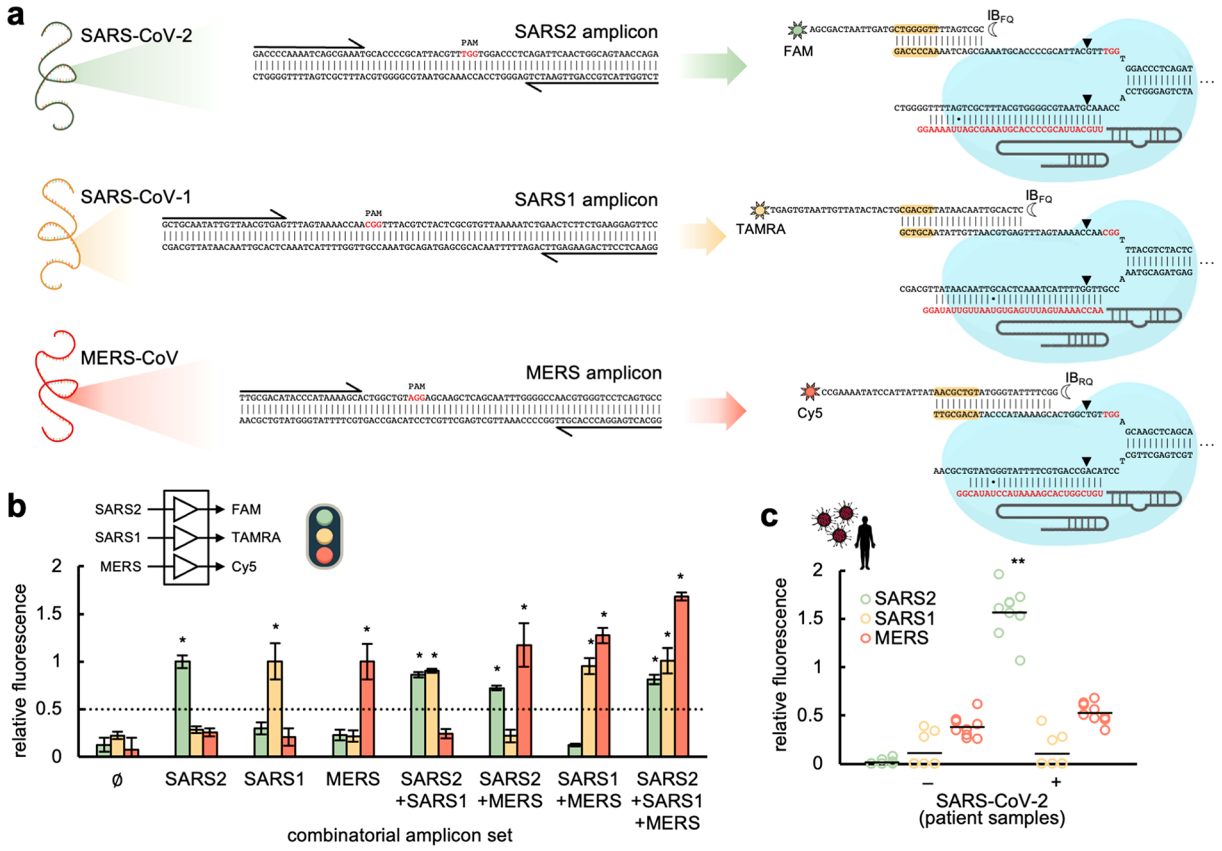

Figure 3. Multiplexed coronavirus detection through CRISPR-Cas9-based strand displacement reactions. (a) Schematics of the global reactions of amplification and detection of DNA products from SARS-CoV-2, SARS-CoV-1, and MERS-CoV (PCR primers drawn at the ends), containing a PAM each (shown in red) for Cas9 recognition. Preassembled CRISPR-Cas9 ribonucleoproteins targeting the amplicons (sgRNA spacers marked in red) and appropriate molecular beacons were used for the detection (seed regions for the beacon-displaced strand interaction marked in yellow). The molecular beacons were labeled with FAM and IB_{FQ} (for SARS-CoV-2 detection), TAMRA and IB_{FQ} (for SARS-CoV-1 detection), and Cy5 and IB_{RQ} (for MERS-CoV detection). Wobble base pairs denoted by dots. (b) Fluorescence-based characterization of the detection by working with combinatorial sets of DNA amplicons. The detection threshold (given by the dotted line) was set to 0.5, indicating that the difference in relative fluorescence was more than 2-fold. (c) Differential detection of SARS-CoV-2 in patient samples (6 patients, 3 reactions per patient); amplifications performed by RT-PCR. Error bars correspond to standard deviations ($n = 3$). *Statistical significance with test samples (Welch's t-test, two-tailed $P < 0.05$, and relative fluorescence > 0.5). **Statistical significance with patient samples (Welch's t-test, two-tailed $P < 0.001$).

fluorescence channels in the case of patients diagnosed as infected by SARS-CoV-2 in the hospital (Figure 2c).

Furthermore, we investigated the possibility of using DETECTR (DNA endonuclease-targeted CRISPR *trans* reporter)[5] in combination with COLUMBO to perform multiplexed detections. The structure of the molecular beacon together with a low concentration regime for Cas12a would prevent a premature degradation of the beacon as a result of the collateral catalytic activity of this nuclease upon targeting. Alternatively, a molecular beacon of RNA could be used. We focused on detecting the DNA amplicon generated with the CDC N1 primers with DETECTR, noting that it contains a PAM for Cas12a binding (TTTV),[7] and the amplicon generated with the Charité E-Sarbeco primers with COLUMBO (Figure 2d). A suitable sgRNA was in vitro transcribed and assembled with the *Acidaminococcus* sp. Cas12a for DETECTR. After multiplexed RT-PCR or RT-RPA amplification over patient samples, we found that COLUMBO and DETECTR can work together to detect different SARS-CoV-2 genes (Figure 2e).

Differential Virus Detection with COLUMBO. We assessed the ability of COLUMBO to detect simultaneously different viruses in the sample. Such a multiplexed detection is important because it may allow performing differential diagnostics in the future and uncovering mixed infections. We focused on three different coronaviruses: SARS-CoV-2, SARS-CoV-1, and Middle East respiratory syndrome coronavirus (MERS-CoV).[27] The CDC N1 primers were considered for SARS-CoV-2, new primers were designed for SARS-CoV-1, and previously designed primers were taken for MERS-CoV.[28] We checked that each pair of primers only aligns with the cognate genome. Suitable PAMs were found in the corresponding amplicons (Figure 3a). We then designed new sgRNAs and beacons to detect SARS-CoV-1 (signal from fluorophore TAMRA) and MERS-CoV (signal from fluorophore Cy5). The low GC content of the protospacer regions in these cases forced the design of beacons with larger stems in order to ensure intra- and intermolecular stability. Notably, COLUMBO allowed the precise detection of the different DNA amplicons added in a combinatorial way, with a minimal 2.4-fold change in relative fluorescence as before (Figure 3b). In addition, we performed a multiplexed RT-PCR amplification over patient samples with all primers. COLUMBO gave a positive signal only in the green fluorescence channel, corresponding to SARS-CoV-2, in the case of patients diagnosed as infected in the hospital (Figure 3c). These

https://doi.org/10.1021/acs.analchem.3c01041
Anal. Chem. XXXX, XXX, XXX−XXX

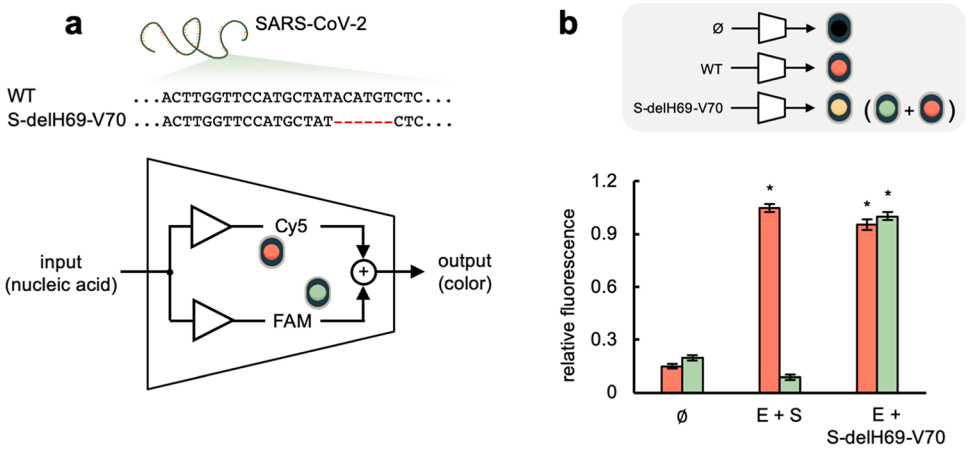

Figure 4. Mutant SARS-CoV-2 detection through CRISPR-Cas9-based strand displacement reactions. (a) Schematics of an electronic circuit implementing a molecular program for detection: if the sample is free of SARS-CoV-2, there is no light signal; if it contains the wild-type SARS-CoV-2, a red signal is obtained (only from Cy5); if it contains a SARS-CoV-2 that carries the mutation S-delH69-V70, red and green signals are obtained (from Cy5 and FAM), i.e., a "yellow" signal. (b) Fluorescence-based characterization of the detection by working directly with DNA amplicons: none, E and S (simulating the wild-type SARS-CoV-2), and E and S-delH69-V70 (simulating a mutant SARS-CoV-2, Alpha variant). Error bars correspond to standard deviations (n = 3). *Statistical significance with test samples (Welch's t-test, two-tailed $P < 0.05$).

results indicate that COLUMBO is a suitable method to achieve a direct multiplexed detection of nucleic acids with no need for gel electrophoresis, in contrast to previous work.[16]

Next, we tested if COLUMBO, in addition to detecting SARS-CoV-2, can reveal specific mutations. This would be important to provide a cost-effective genetic perspective about the transmission dynamics in the pandemic.[29] We hypothesized that it could be possible to perform a multiplexed detection with two sgRNAs, one targeting a conserved region to confirm the infection by SARS-CoV-2 and another targeting a mutable region to identify a specific viral genotype (Figure 4a). Mutations in the PAM would compromise the binding of the Cas protein, while mutations in the protospacer the binding of the beacon (in the PAM-distal region) and the sgRNA (in the PAM-proximal region; Figure S8). As a proof of concept, we here focused on the H69-V70 deletion of six nucleotides in the S gene (S-delH69-V70) identified in the Alpha variant.[30] Using test samples containing the E and S/S-delH69-V70 amplicons, the intended multiplexed detection was successfully accomplished, indicating that the corresponding sgRNA does not interact with the wild-type S amplicon (Figure 4b). We also considered a deletion of three nucleotides in the N gene (N-delQ9) identified in a Delta variant sublineage,[31] which we were able to detect in a multiplexed fashion using test samples containing the E and N1/N1-delQ9 amplicons (Figure S9). These examples suggest that, provided suitable sgRNAs and beacons are designed, COLUMBO could be applied to identify further SARS-CoV-2 mutants to limit the use of sequencing.

Biocomputational Virus Detection with COLUMBO. The lack of collateral cleavage activity of the nuclease in our detection platform represents an advantage to couple it with DNA computing,[32] thereby going beyond the simple detection paradigm. To illustrate this approach, we designed two molecular programs implementing Boolean logic gates to process combinatorial DNA amplicons from SARS-CoV-2 (we focused on the N1 and E amplicons). First, we designed an OR gate (Figure 5a), aimed at producing a fluorescence signal when there is at least one amplicon in the reaction. The assembly of three ssDNA molecules with a partial complementary among them led to a stable nonregular structure capable of specifically interacting with the displaced strands generated by the sgRNA-Cas9 ribonucleoproteins upon targeting. These ssDNA molecules were appropriately labeled with the fluorophore Cy5 or the dark quencher IB_{RQ} to achieve the intended logic behavior. The engineered system performed well with DNA amplicons as inputs, showing a dynamic range of an almost 3-fold change in red fluorescence (Figure 5b). In the absence of the sgRNA-Cas9 ribonucleoproteins, the system was irresponsive. Moreover, we assayed the system with amplified products from patient samples, finding similar results (Figure 5c). As expected, the computation only took place when using positive patient samples.

Second, we designed an AND gate (Figure 5d), aimed at producing a fluorescence signal only when the two amplicons are present in the reaction. The very same nucleotide sequences of those ssDNA molecules used to implement the OR gate were used, but the labeling with the fluorophore Cy5 and the dark quencher IB_{RQ} changed. In this case, two quenchers and one internal fluorophore were used to achieve the intended logic behavior. The response of the engineered system with DNA amplicons as inputs showed a dynamic range of 3-fold change in red fluorescence (Figure 5e). We noted, however, that the system slightly responded to just one input. As before, in the absence of the sgRNA-Cas9 ribonucleoproteins, the system was irresponsive. Moreover, the assay of the system with amplified products from patient samples revealed similar results (Figure 5f), although in this case the maximal fluorescence level was reduced. Overall, these results highlight the utility of the CRISPR-Cas9 system to connect a specific and sensitive virus detection with the ability to compute using DNA as a substrate, which might lead to more complex in vitro diagnostic programs.

DISCUSSION

We have enlarged the CRISPR-based detection toolkit with the CRISPR-Cas9 system on which COLUMBO relies. As in the case of SHERLOCK (specific high-sensitivity enzymatic reporter unlocking)[4] and DETECTR,[5] a preamplification process is required. However, COLUMBO is based on strand

https://doi.org/10.1021/acs.analchem.3c01041
Anal. Chem. XXXX, XXX, XXX−XXX

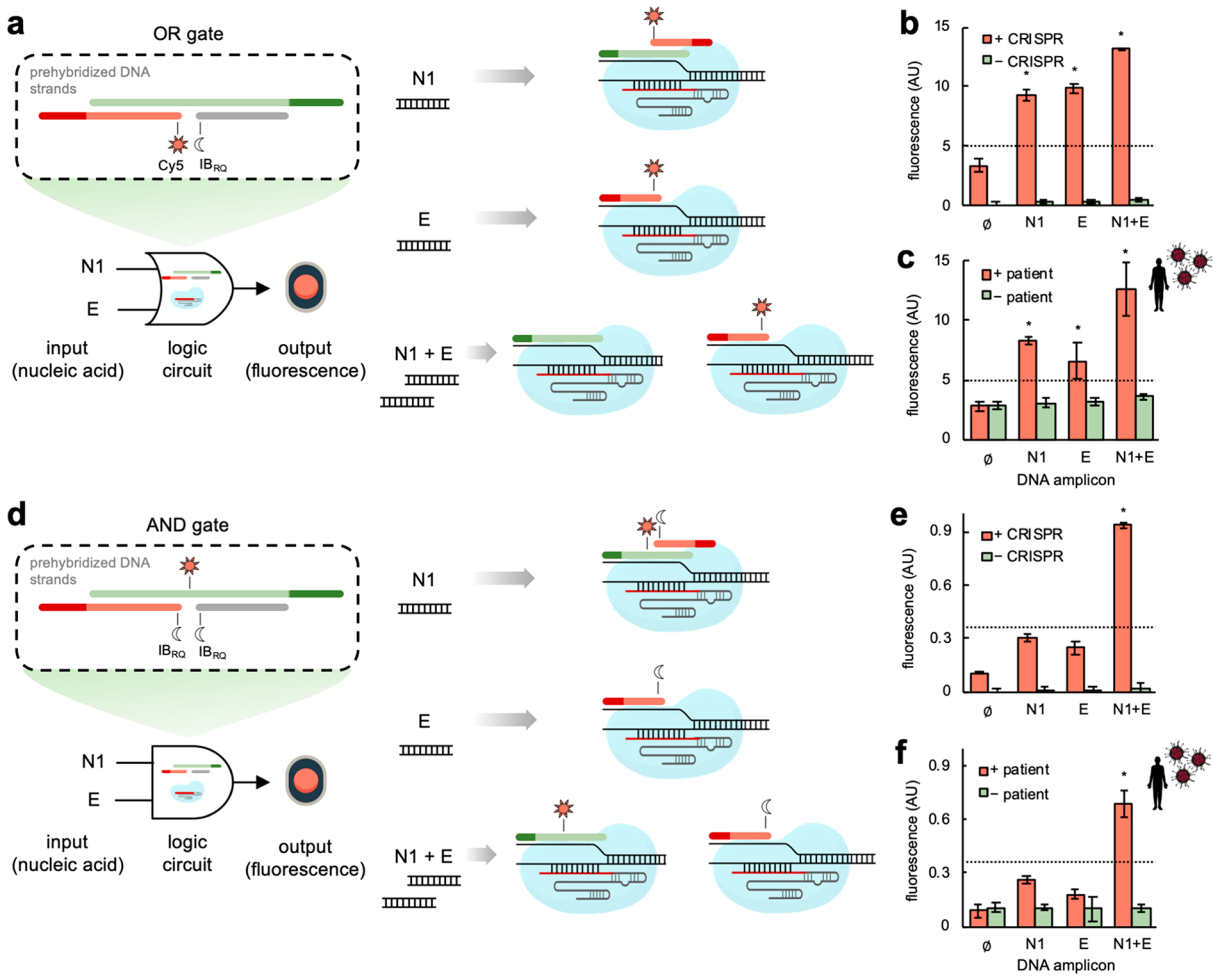

Figure 5. Biocomputational SARS-CoV-2 detection through CRISPR-Cas9-based strand displacement reactions. (a) Schematics of the OR logic circuit. Three prehybridized oligonucleotides conform the OR gate, which can interact with the CRISPR complexes formed upon detection of the virus-derived DNA amplicons (N1 and E). In this case, the red strand was labeled with Cy5 in its 5′ end and the gray strand with IB_{RQ} in its 3′ end. The dark green and red regions represent the toeholds seeding the interactions with the corresponding CRISPR complexes (the green strand interacts with the displaced strand of the N1 amplicon, while the red strand does with the displaced strand of the E amplicon). On the left, schematics of the biocomputation reactions in response to one or two DNA amplicons. (b) Fluorescence-based characterization of the OR gate performance with DNA amplicons. (c) Biocomputation using patient samples (2 patients, 3 reactions per patient). (d) Schematics of the AND logic circuit. As before, three prehybridized oligonucleotides conform the AND gate. In this case, the green strand was labeled with Cy5 internally, the red strand with IB_{RQ} in its 5′ end, and the gray strand with IB_{RQ} in its 3′ end. On the left, schematics of the biocomputation reactions in response to one or two DNA amplicons. (e) Fluorescence-based characterization of the AND gate performance with DNA amplicons. (f) Biocomputation using patient samples. The detection threshold (given by the dotted line) was set to 5 in (b) and (c) and 0.35 in (e) and (f). Amplifications performed by RT-PCR in (c) and (f). Error bars correspond to standard deviations (n = 3). *Statistical significance (Welch's t-test, two-tailed $P < 0.05$). (b) and (c) are determined with respect to the first condition, while (e) and (f) are determined with respect to the first three conditions.

displacement (hybridization) and not on a collateral catalytic activity. That is, the sgRNA-Cas9 ribonucleoprotein gives the specificity of the detection by targeting the resulting DNA amplicon, and the interaction between the displaced DNA strand and a molecular beacon gives the fluorescence readout. Consequently, different DNA amplicons can be detected with the same nuclease (Cas9) and without the need for complex setups to run parallel microreactions,[14,15] which is an advance in terms of broad usability and standardization. Remarkably, we have applied this novel approach with success to detect SARS-CoV-2 in patient samples, thereby envisioning a diagnostic potential. We also showed that COLUMBO and DETECTR can work together, a feature that is important to boost the intricacy in CRISPR diagnostics.

In our designer scheme, the native Cas9 from *S. pyogenes* is exploited, but the use of engineered versions of Cas9 with enhanced specificity[33] could make the detection of virus variants with subtle specific mutations more plausible. COLUMBO might be run after RT-qPCR completion as a simple virus genotyping step in order to complement the quantitative detection in the clinic with relevant information for patient prognosis and epidemiological surveillance. Further work should also refine the approach to make it even more streamlined (i.e., joining amplification and detection). On the other hand, increasing developments on portable fluorescence microscopy coupled to mobile phones, already applied to detect SARS-CoV-2,[12,34] are appealing and might be used to characterize our CRISPR-Cas9 reactions. A cell-free expression system might also be interfaced to achieve a detection with a

https://doi.org/10.1021/acs.analchem.3c01041
Anal. Chem. XXXX, XXX, XXX−XXX

colorimetric readout,[35] given that strand displacement allows nucleic acid conversion.[17] This would enable point-of-care diagnostics and field-deployable testing.

Finally, we envision the application of computational methods to automate the sequence design of the different nucleic acid species that COLUMBO requires, given a series of energetic and structural specifications.[36,37] This would allow ending with species with suitable intra- and intermolecular stability, while minimizing undesired cross-interactions (e.g., between the molecular beacon and the sgRNA). One limitation of COLUMBO is the sometimes-moderate dynamic range of the fluorescence signal, which may make it difficult to achieve an accurate detection of the virus, especially in the case of multiplexing. In this regard, the combination of computational sequence design with systematic functional screening might allow optimizing the system. In addition, computational methods might contribute to the engineering of more complex nucleic acid circuits not only to detect a specific sequence, but to perform a logic computation from multiple input signals (e.g., to inform about the presence of two or more viruses in the sample with just one fluorophore).[32] Within this extended diagnostic framework, the activity of the sgRNAs might be conditional to the presence or absence of further strands to have an additional layer of operation.[38] All in all, due to its specificity, multiplexing capability, compatibility, and easy usage, we expect COLUMBO to provide exciting prospects in the field of viral diagnostics and DNA/RNA-based computation.

METHODS

Test Samples. For single detection, a test sample was generated with a plasmid containing the SARS-CoV-2 E gene (IDT) at 10^3 copies/μL (different dilutions down to 1 copy/μL were also made). Additional test samples were generated for multiplexed detection. First, a test sample was generated by mixing two plasmids containing the SARS-CoV-2 N and E genes (IDT) each at 10^3 copies/μL. Second, different combinatorial samples of three DNA amplicons from different viruses were prepared. The DNA amplicon from SARS-CoV-2 was generated by PCR from the aforementioned plasmid with the CDC N1 primers, and the DNA amplicons from SARS-CoV-1 and MERS-CoV were chemically synthesized (IDT). Third, two DNA amplicons from the S gene, one being the wild-type version and another carrying the amino acid H69-V70 deletion,[30] and a DNA amplicon from the N gene carrying the CAG deletion at position 28298 (deleting the ninth residue Q)[31] were chemically synthesized.

Patient Samples. Nasopharyngeal swabs corresponding to infected and noninfected patients with SARS-CoV-2 (RT-qPCR diagnostics) were obtained from the Clinic University Hospital of Valencia (Spain). Samples were inactivated by heat shock (30 min at 60 °C) before proceeding. No RNA extraction was performed. The ethical committee of the Clinic University Hospital approved this study (order #2020/221).

Primers. The CDC N1 and N2 primers were used to amplify two different N gene regions from SARS-CoV-2, and the Charité E-Sarbeco primers were used to amplify one E gene region.[23] The Charité E-Sarbeco primers were used for both PCR and RPA, while the CDC N1 primers were only used for PCR. Longer primers targeting the N1 region were designed for RPA. Primers to amplify the S gene were also designed here. In addition, a genomic region from SARS-CoV-1 could be amplified with newly designed primers, and a region from MERS-CoV could be amplified with the previously designed MERS-related N2 primers.[28] Sequences are provided in Data set S1.

CRISPR Elements. Three versions of *S. pyogenes* Cas9 were used (from IDT): the wild-type nuclease (Cas9), the Cas9 H840A nickase (Cas9n), and the catalytically dead Cas9 protein (dCas9).[24] *Acidaminococcus* sp. Cas12a (from IDT) was also used to implement DETECTR reactions. In addition, sgRNAs were generated by in vitro transcription with the TranscriptAid T7 high yield transcription kit (Thermo) from DNA templates. sgRNAs were then purified by using the RNA clean and concentrator column (Zymo) and quantified in a NanoDrop. Sequences are provided in Data set S1.

Molecular Beacons. Different DNA oligonucleotides folding into a stem-loop structure and appropriately labeled were designed to hybridize with the displaced DNA strands from the CRISPR reactions. These probes were designed to have a seed region in the loop and of high GC content, as well as a melting temperature higher than 50 °C (Figure S10 shows a computational study on the size of the seed region). The correct folding and hybridization ability (with the target DNA, but not with the sgRNA) were checked with NUPACK.[37] Molecular beacons targeting the PAM-distal region were labeled in their 5′ end with a dark quencher (lB_{FQ} or lB_{RQ}) and in their 3′ end with a fluorophore (FAM, TAMRA, or Cy5). When targeting the PAM-proximal region, the beacon was labeled in its 5′ end with FAM and its 3′ end with lB_{FQ} or Black Hole Quencher 1 (BHQ1). To ensure appropriate folding, molecular beacons were heated at 95 °C for 2 min and then cooled slowly to 25 °C prior to their use in the CRISPR reactions. Sequences provided in the Data set S1.

Nucleic Acid Amplification by PCR. With test samples, 250 nM of forward and reverse primers, 200 μM dNTPs (NZYTech), 0.02 U/μL Phusion high-fidelity DNA polymerase (Thermo), 1× Phusion buffer, and 2 μL of sample were mixed for a total volume of 20 μL (adjusted with RNase-free water). The protocol was 98 °C for 30 s for denaturation, followed by 35 cycles of 98 °C for 10 s, 62 °C for 10 s, and 72 °C for 5 s for amplification. With patient samples, the TaqPath 1-step RT-qPCR master mix, CG (Applied) was used with 250 nM of forward and reverse primers and 4 μL of sample. The protocol was 50 °C for 15 min for RT, then 95 °C for 2 min for denaturation, followed by 35 cycles of 95 °C for 15 s and 62 °C for 60 s for amplification. In the case of multiplexed amplifications, each primer pair was also used at 250 nM. Reactions were incubated in a thermocycler (Eppendorf). PCR products were purified by using a DNA clean and concentrator column (Zymo) by centrifugation.

Nucleic Acid Amplification by RPA. The TwistAmp basic kit (TwistDX) was used. With test samples, 480 nM of forward and reverse primers was added to 29.5 μL of rehydration buffer for a total volume of 45.4 μL (adjusted with RNase-free water). With patient samples, 500 U RevertAid (Thermo) and 50 U RNase inhibitor (Thermo) were added to the mix. In the case of multiplexed amplifications, each primer pair was used at 240 nM. The TwistAmp basic reaction pellet was resuspended with the resulting volume, and then 2 μL of the sample was added. To start the reaction, 280 mM magnesium acetate was added. Reactions were incubated at 42 °C for 30 min in a thermomixer (Eppendorf), shaking 10 s at 300 rpm every 2 min. RPA products were purified by using the DNA clean and concentrator column by centrifugation.

https://doi.org/10.1021/acs.analchem.3c01041
Anal. Chem. XXXX, XXX, XXX−XXX

CRISPR-Cas9-Based Detection. CRISPR reactions were performed in 1× TAE buffer pH 8.5 (Invitrogen), 0.05% Tween 20 (Merck), and 12.5 mM $MgCl_2$ (Merck) at a final volume of 20 μL. The CRISPR-Cas9 ribonucleoprotein, previously assembled at room temperature for 30 min, was added at 100 nM. In the case of test samples, 40 nM of amplified DNA (otherwise specified) was used per reaction. In the case of patient samples, 2 or 6 μL of amplified product was used per reaction for single or multiplexed detection. For the limit of detection assays, 2 μL of purified PCR product was used (5 μL in the case of RPA). Reactions were incubated at 37 °C for 20 min in a thermomixer (Eppendorf). The molecular beacon (beacons) was (were) added afterward at 100 nM, followed by 5 min incubation at 37 °C. The beacons could also be added at the beginning of the CRISPR reaction to simplify the approach, obtaining similar results (Figure S5b). For the multiplexed detection of the E and S-delH69-V70 amplicons, 200 nM of ribonucleoprotein targeting the S-delH69-V70 amplicon was used, and the two beacons were added at the beginning.

Combined CRISPR-Cas9- and CRISPR-Cas12a-Based Detection. CRISPR reactions were performed in 1× TAE buffer pH 8.5 (Invitrogen), 0.05% Tween 20 (Merck), and 12.5 mM $MgCl_2$ (Merck) at a final volume of 20 μL. The CRISPR-Cas9 and CRISPR-Cas12a ribonucleoproteins, previously assembled at room temperature for 30 min, were added at 100 and 1.33 nM, respectively. The ssDNA probe for CRISPR-Cas12a (TTATT, labeled in its 5′ end with the fluorophore FAM and in its 3′ end with the dark quencher IB_{FQ}) was also added at 100 nM. From patient samples, 4 μL of the amplified product was used per reaction for multiplexed detection. Reactions were incubated at 37 °C for 20 min in a thermomixer (Eppendorf). The molecular beacon was added afterward at 100 nM, followed by a 5 min incubation at 37 °C.

Biocomputing Coupled to CRISPR-Cas9-Based Detection. DNA logic circuits implementing OR and AND gates were engineered. Each gate was formed by three different ssDNA molecules that were chemically synthesized (IDT) with appropriate fluorophore (Cy5) or dark quencher (IB_{RQ}) labels. The ssDNA sequences were the same for the OR and AND gates, only changed the fluorophore/quencher labeling. The strand displacement ability was checked with NUPACK. The hybridizing ssDNA molecules forming the gates were designed to have toeholds to seed the interactions with the displaced strands of the targeted DNA amplicons (N1 and E) and to form a stable complex at 37 °C. Prior to their use in the CRISPR reactions, the three strands implementing a gate were heated at 95 °C for 2 min and then cooled slowly to 25 °C. The logic circuits were assayed for functionality with appropriate oligonucleotides as inputs (Figure S11). Sequences provided in the Data set S1. CRISPR reactions were performed in 1× TAE buffer pH 8.5 (Invitrogen), 0.05% Tween 20 (Merck), and 12.5 mM $MgCl_2$ (Merck) at a final volume of 20 μL. The CRISPR-Cas9 ribonucleoprotein, previously assembled at room temperature for 30 min, was added at 100 nM, except the ribonucleoprotein targeting the N1 amplicon in the OR gate, which was added at 200 nM. Input DNA amplicons (N1 and E) were mixed in a combinatorial way, 40 nM of each one if obtained from test samples or 2 μL of each amplified product if obtained from patient samples. The prehybridized gate was added at 200 nM. Reactions were incubated at 37 °C for 1 h in a thermomixer (Eppendorf).

RT-qPCR. The TaqPath 1-step RT-qPCR master mix, CG was used. Two μL of sample was mixed with 500 nM of forward and reverse primers (CDC N1), 250 nM of ssDNA probe (provided by IDT to detect the N gene), and 5 μL of the master mix for a total volume of 20 μL (adjusted with RNase-free water) in a fast microplate (Applied). Reactions were performed in a QuantStudio 3 equipment (Thermo) with this protocol: incubation at 25 °C for 2 min for uracil-N glycosylation, followed by 50 °C for 15 min for RT, followed by an inactivation step at 90 °C for 2 min, then followed by 40 cycles of amplification at 90 °C for 3 s and 60 °C for 30 s.

Gel Electrophoresis. Nucleic acid amplification (from plasmid or viral genome) was confirmed by gel electrophoresis (see examples in Figure S12). For that, 2 μL of amplified product was used. Gel electrophoresis was also used to confirm the interaction between the molecular beacon and the displaced strand from the DNA amplicon (ssDNA molecule). For that, the nucleic acid species were introduced at 7.5 μM each in 20 μL of the CRISPR reaction buffer and were incubated for 30 min at room temperature. Samples were loaded on a 3% agarose gel prepared with 0.5× TBE buffer, which was run for 45 min at room temperature (110 V). Gels were stained using RealSafe (Durviz). The GeneRuler ultralow range DNA ladder (10-300 bp, Thermo) was used as a marker.

Fluorometry. Reaction volumes were loaded in a black 384-well microplate with clear bottom (Falcon), which was then placed in a fluorometer (Varioskan Lux, Thermo) to measure green, orange, and red fluorescence (measurement time of 100 ms, automatic range, and top optics). For FAM, excitation was at 495/12 nm and emission at 520/12 nm (green); for TAMRA, excitation was at 557/12 nm and emission at 583/12 nm (orange); and for Cy5, excitation was at 645/12 nm and emission at 670/12 nm (red). Fluorescence values were represented as absolute or relative. For the latter, the fluorescence values of the closed-form beacons were subtracted to correct the signals, which were then normalized by appropriate reference values. In the case of multiplexed reactions for the simultaneous detection of different SARS-CoV-2 genes or different coronaviruses, the normalization was with respect to the positive case where only one amplicon is present. In the case of reactions for mutant SARS-CoV-2 detection or combining Cas9 and Cas12a, the normalization was with respect to the positive case where all amplicons are present.

■ ASSOCIATED CONTENT

Supporting Information

The Supporting Information is available free of charge at https://pubs.acs.org/doi/10.1021/acs.analchem.3c01041.

Experimental notes providing additional detail on the design and characterization of the engineered molecular systems. Additional figures showing control experiments and further activity assays (PDF)

Nucleotide sequences of the elements used in this work (XLSX)

■ AUTHOR INFORMATION

Corresponding Author

Guillermo Rodrigo − *Institute for Integrative Systems Biology (I2SysBio), CSIC − University of Valencia, 46980 Paterna, Spain;* orcid.org/0000-0002-1871-9617; Email: guillermo.rodrigo@csic.es

https://doi.org/10.1021/acs.analchem.3c01041
Anal. Chem. XXXX, XXX, XXX−XXX

Authors

Rosa Márquez-Costa − *Institute for Integrative Systems Biology (I2SysBio), CSIC − University of Valencia, 46980 Paterna, Spain;* orcid.org/0000-0001-9956-0873

Roser Montagud-Martínez − *Institute for Integrative Systems Biology (I2SysBio), CSIC − University of Valencia, 46980 Paterna, Spain*

María-Carmen Marqués − *Institute for Integrative Systems Biology (I2SysBio), CSIC − University of Valencia, 46980 Paterna, Spain*

Eliseo Albert − *Microbiology Service, Clinic University Hospital, INCLIVA Biomedical Research Institute, 46010 Valencia, Spain*

David Navarro − *Microbiology Service, Clinic University Hospital, INCLIVA Biomedical Research Institute, 46010 Valencia, Spain; Department of Microbiology, School of Medicine, University of Valencia, 46010 Valencia, Spain*

José-Antonio Daròs − *Instituto de Biología Molecular y Celular de Plantas (IBMCP), CSIC − Universitat Politècnica de València, 46022 Valencia, Spain;* orcid.org/0000-0002-6535-2889

Raúl Ruiz − *Institute for Integrative Systems Biology (I2SysBio), CSIC − University of Valencia, 46980 Paterna, Spain*

Complete contact information is available at: https://pubs.acs.org/10.1021/acs.analchem.3c01041

Author Contributions

#These authors contributed equally to this work.

Notes

The authors declare the following competing financial interest(s): R.M.C., R.M.M., R.R., and G.R. declare that they are patenting the detection method presented in this work.

■ ACKNOWLEDGMENTS

This work was supported by the Fondo Supera Covid-19 from CRUE and Banco Santander (Grant COV-CRISPIS to G.R.), the CSIC PTI Salud Global (Grant SGL2021-03-040 to G.R.) through the NextGenerationEU Fund (regulation 2020/2094), the Spanish Ministry of Science and Innovation (Grants PGC2018-101410-B-I00 to G.R. and PID2020-114691RB-I00 to J.A.D., both cofinanced by the European Regional Development Fund), and the Regional Government of Valencia (Grants SEJI/2020/011 and GVA-COVID19/2021/036 to G.R.). R.M.C. was supported by a predoctoral fellowship from the Spanish Ministry of Science and Innovation (PRE2019-088531). Publication fees covered by the CSIC Open Access Publication Support Program.

■ REFERENCES

(1) Zhu, N.; Zhang, D.; Wang, W.; Li, X.; Yang, B.; Song, J.; Zhao, X.; Huang, B.; Shi, W.; Lu, R.; Niu, P.; Zhan, F.; Ma, X.; Wang, D.; Xu, W.; Wu, G.; Gao, G. F.; Tan, W. *N Engl J. Med.* **2020**, *382*, 727−733.

(2) Yang, S.; Rothman, R. E. *Lancet Infect Dis* **2004**, *4*, 337−348.

(3) Mina, M. J.; Parker, R.; Larremore, D. B. *N Engl J. Med.* **2020**, *383*, No. e120.

(4) Gootenberg, J. S.; Abudayyeh, O. O.; Lee, J. W.; Essletzbichler, P.; Dy, A. J.; Joung, J.; Verdine, V.; Donghia, N.; Daringer, N. M.; Freije, C. A.; Myhrvold, C.; Bhattacharyya, R. P.; Livny, J.; Regev, A.; Koonin, E. V.; Hung, D. T.; Sabeti, P. C.; Collins, J. J.; Zhang, F. *Science* **2017**, *356*, 438−442.

(5) Chen, J. S.; Ma, E.; Harrington, L. B.; Da Costa, M.; Tian, X.; Palefsky, J. M.; Doudna, J. A. *Science* **2018**, *360*, 436−439.

(6) Zhao, Y.; Chen, F.; Li, Q.; Wang, L.; Fan, C. *Chem. Rev.* **2015**, *115*, 12491−12545.

(7) Broughton, J. P.; Deng, X.; Yu, G.; Fasching, C. L.; Servellita, V.; Singh, J.; Miao, X.; Streithorst, J. A.; Granados, A.; Sotomayor-Gonzalez, A.; Zorn, K.; Gopez, A.; Hsu, E.; Gu, W.; Miller, S.; Pan, C. Y.; Guevara, H.; Wadford, D. A.; Chen, J. S.; Chiu, C. Y. *Nat. Biotechnol.* **2020**, *38*, 870−874.

(8) Ding, X.; Yin, K.; Li, Z.; Lalla, R. V.; Ballesteros, E.; Sfeir, M. M.; Liu, C. *Nat. Commun.* **2020**, *11*, 4711.

(9) Xiong, D.; Dai, W.; Gong, J.; Li, G.; Liu, N.; Wu, W.; Pan, J.; Chen, C.; Jiao, Y.; Deng, H.; Ye, J.; Zhang, X.; Huang, H.; Li, Q.; Xue, L.; Zhang, X.; Tang, G. *PLoS Biol.* **2020**, *18*, No. e3000978.

(10) Patchsung, M.; et al. *Nat. Biomed Eng.* **2020**, *4*, 1140−1149.

(11) Arizti-Sanz, J.; et al. *Nat. Commun.* **2020**, *11*, 5921.

(12) Fozouni, P.; et al. *Cell* **2021**, *184*, 323−333.

(13) Gootenberg, J. S.; Abudayyeh, O. O.; Kellner, M. J.; Joung, J.; Collins, J. J.; Zhang, F. *Science* **2018**, *360*, 439−444.

(14) Ackerman, C. M.; Myhrvold, C.; Thakku, S. G.; Freije, C. A.; Metsky, H. C.; Yang, D. K.; Ye, S. H.; Boehm, C. K.; Kosoko-Thoroddsen, T. F.; Kehe, J.; Nguyen, T. G.; Carter, A.; Kulesa, A.; Barnes, J. R.; Dugan, V. G.; Hung, D. T.; Blainey, P. C.; Sabeti, P. C. *Nature* **2020**, *582*, 277−282.

(15) Tian, T.; Shu, B.; Jiang, Y.; Ye, M.; Liu, L.; Guo, Z.; Han, Z.; Wang, Z.; Zhou, X. *ACS Nano* **2021**, *15*, 1167−1178.

(16) Jiao, C.; Sharma, S.; Dugar, G.; Peeck, N. L.; Bischler, T.; Wimmer, F.; Yu, Y.; Barquist, L.; Schoen, C.; Kurzai, O.; Sharma, C. M.; Beisel, C. L. *Science* **2021**, *372*, 941−948.

(17) Montagud-Martinez, R.; Heras-Hernandez, M.; Goiriz, L.; Daros, J. A.; Rodrigo, G. *ACS Synth. Biol.* **2021**, *10*, 950−956.

(18) Tyagi, S.; Kramer, F. R. *Nat. Biotechnol.* **1996**, *14*, 303−308.

(19) Piepenburg, O.; Williams, C. H.; Stemple, D. L.; Armes, N. A. *PLoS Biol.* **2006**, *4*, No. e204.

(20) Richardson, C. D.; Ray, G. J.; DeWitt, M. A.; Curie, G. L.; Corn, J. E. *Nat. Biotechnol.* **2016**, *34*, 339−344.

(21) Rodrigo, G.; Landrain, T. E.; Shen, S.; Jaramillo, A. *Trends Genet* **2013**, *29*, 529−536.

(22) Chen, F.; Ding, X.; Feng, Y.; Seebeck, T.; Jiang, Y.; Davis, G. D. *Nat. Commun.* **2017**, *8*, 14958.

(23) Vogels, C. B.; et al. *Nat. Microbiol* **2020**, *5*, 1299−1305.

(24) Jinek, M.; Chylinski, K.; Fonfara, I.; Hauer, M.; Doudna, J. A.; Charpentier, E. *Science* **2012**, *337*, 816−821.

(25) Manghi, M.; Destainville, N. *Phys. Rep.* **2016**, *631*, 1−41.

(26) Torres, I.; Qualai, J.; Albert, E.; Bueno, F.; Huntley, D.; Poujois, S.; Gil, M. T.; Navarro, D. *J. Med. Virol* **2021**, *93*, 5233−5235.

(27) da Costa, V. G.; Moreli, M. L.; Saivish, M. V. *Arch. Virol.* **2020**, *165*, 1517−1526.

(28) Lu, X.; Whitaker, B.; Sakthivel, S. K. K.; Kamili, S.; Rose, L. E.; Lowe, L.; Mohareb, E.; Elassal, E. M.; Al-sanouri, T.; Haddadin, A.; Erdman, D. D. *J. Clin Microbiol* **2014**, *52*, 67−75.

(29) du Plessis, L.; et al. *Science* **2021**, *371*, 708−712.

(30) Meng, B.; et al. *Cell Rep* **2021**, *35*, 109292.

(31) Wang, H.; Jean, S.; Wilson, S. A.; Lucyshyn, J. M.; McGrath, S.; Wilson, R. K.; Magrini, V.; Leber, A. L. *Diagn Microbiol Infect Dis* **2022**, *102*, 115631.

(32) Seelig, G.; Soloveichik, D.; Zhang, D. Y.; Winfree, E. *Science* **2006**, *314*, 1585−1588.

(33) Slaymaker, I. M.; Gao, L.; Zetsche, B.; Scott, D. A.; Yan, W. X.; Zhang, F. *Science* **2016**, *351*, 84−88.

(34) Ning, B.; Yu, T.; Zhang, S.; Huang, Z.; Tian, D.; Lin, Z.; Niu, A.; Golden, N.; Hensley, K.; Threeton, B.; Lyon, C. J.; Yin, X. M.; Roy, C. J.; Saba, N. S.; Rappaport, J.; Wei, Q.; Hu, T. Y. *Sci. Adv.* **2021**, *7*, No. eabe3703.

(35) Pardee, K.; Green, A. A.; Takahashi, M. K.; Braff, D.; Lambert, G.; Lee, J. W.; Ferrante, T.; Ma, D.; Donghia, N.; Fan, M.; Daringer, N. M.; Bosch, I.; Dudley, D. M.; O'Connor, D. H.; Gehrke, L.; Collins, J. J. *Cell* **2016**, *165*, 1255−1266.

(36) Rodrigo, G.; Landrain, T. E.; Majer, E.; Daros, J. A.; Jaramillo, A. *PLoS Comput. Biol.* **2013**, *9*, No. e1003172.
(37) Zadeh, J. N.; Steenberg, C. D.; Bois, J. S.; Wolfe, B. R.; Pierce, M. B.; Khan, A. R.; Dirks, R. M.; Pierce, N. A. *J. Comput. Chem.* **2011**, *32*, 170−173.
(38) Li, Y.; Teng, X.; Zhang, K.; Deng, R.; Li, J. *Anal. Chem.* **2019**, *91*, 3989−3996.

https://doi.org/10.1021/acs.analchem.3c01041
Anal. Chem. XXXX, XXX, XXX−XXX